

# Phase formation and characterization of [Fe, Mg]NbO<sub>4</sub> as a new precursor for the PMN–PFN system

N. S. ALMODÓVAR, R. FONT, J. PORTELLES, O. RAYMOND

*Facultad de Física, IMRE, Universidad de la Habana, San Lázaro y L, Vedado, la Habana 10400, Cuba*

J. M. SIQUEIROS

*Centro de Ciencias de la Materia Condensada, UNAM, Apartado Postal 2681, Ensenada, B. C. México, 22800*

*E-mail: [jesus@ccmc.unam.mx](mailto:jesus@ccmc.unam.mx)*

An X-ray diffraction (XRD) and scanning electron microscopy (SEM) study of the phase composition and microstructure characteristics of the  $\text{Mg}_{(1-x)/3}\text{Nb}_{(4-x)/6}\text{Fe}_{x/2}\text{O}_2$  ( $x = 0.5$ ) chemical compound is presented. The samples were prepared by the conventional ceramic method and subjected to different heat treatments. Columbite ( $\text{MgNb}_2\text{O}_6$ ) and iron niobium oxide ( $\text{FeNbO}_4$ , Wolframite) were identified as intermediate compounds in the reaction. A new single phase precursor for the  $(1-x)\text{Pb}(\text{Mg}_{1/3}\text{Nb}_{2/3})\text{O}_3$ - $x\text{Pb}(\text{Fe}_{1/2}\text{Nb}_{1/2})\text{O}_3$  (PMN–PFN) system identified as  $[\text{Fe}, \text{Mg}]\text{NbO}_4$ , was obtained, isostructural with the  $\text{FeNbO}_4$  where Fe and Mg ions occupy the same crystal site (space group  $P1\ 2/a\ 1$ ). From the Rietveld refinement method the cell parameters of the monoclinic structure were determined. The microstructure analysis indicates that the particles are irregular in shape and the grain size tends to increase with the calcination temperature. © 2002 Kluwer Academic Publishers

## 1. Introduction

Lead-based complex perovskites with the general formula  $A(\text{B}'\text{B}'')\text{O}_3$ , such as  $\text{Pb}(\text{Mg}_{1/3}\text{Nb}_{2/3})\text{O}_3$ , (PMN);  $\text{Pb}(\text{Fe}_{1/2}\text{Nb}_{1/2})\text{O}_3$ , (PFN);  $\text{Pb}(\text{Zn}_{1/3}\text{Nb}_{2/3})\text{O}_3$ , (PZN) and  $\text{Pb}(\text{Fe}_{2/3}\text{W}_{1/3})\text{O}_3$ , (PFW) have received considerable attention for many years due to their high dielectric constants, diffuse phase transition characteristics and relatively low sintering temperature compared with barium titanate. These compounds have found many practical applications in areas such as multilayer ceramic capacitors (MLCC), actuators, pyroelectric detectors, piezoelectric transducers, etc. [1–3]. In particular, PFN is a relaxor ferroelectric with interesting properties such as high dielectric constant and high Curie temperature together with large spontaneous polarization making it a good candidate for non-volatile memory applications [4–6].

Recently, much attention has been paid to obtaining powders with small particle sizes using sol-gel [7], coprecipitation [8, 9] and combustion [10] techniques as alternative procedures. However, for many years, the traditional ceramic technique has been the corner stone for the world production of ferroelectric materials due to low cost, simple processing and suitable dielectric properties for practical applications. In general, this technique involves powder preparation, pressing into a pellet and sintering. It is well known that starting powders and heat treatments have an important role in the

desired phase formation, structure and dielectric properties of the final product [11, 12]. In the case of the PMN–PFN system the preparation of single-phase material is very difficult due to the high volatility of Pb and the segregation of a secondary pyrochlore phase that has a considerable negative effect on the dielectric properties of the final compound. In this sense several modifications to the traditional ceramic method have been made to enhance the PMN–PFN phase yield by using a B-site precursor method [11–15]. This method has been successfully used in the preparation of single phase PMN–PFN [13].

Recent work [12, 16–18] has confirmed the successful preparation of single phase PMN and PFN employing intermediate phases of  $\text{MgNb}_2\text{O}_6$  and  $\text{FeNbO}_4$  as precursor compounds. Sun-Gon Jun *et al.* [13] report single phase  $(1-x)\text{PMN}-x\text{PFN}$  ( $0 \leq x \leq 1$ ) prepared using B-site precursor powders of  $(1-x)\text{Mg}_{1/3}\text{Nb}_{2/3}\text{O}_2-x(\text{Fe}_{1/2}\text{Nb}_{1/2})\text{O}_2$ . These authors report the presence of columbite ( $\text{MgNb}_2\text{O}_6$ ) and ferrocolumbite ( $\text{FeNbO}_4$ ) in the case of pure precursors ( $x = 0$ ,  $x = 1$ ) but a detailed discussion about the intermediate composition is missing. The aim of this work is to use of x-ray diffraction (XRD) and scanning electron microscopy (SEM) to study the reaction kinetics, phase composition and optimal sintering conditions of a new single phase precursor for 0.5PMN–0.5PFN starting from  $\text{Mg}_{(1-x)/3}\text{Nb}_{(4-x)/6}\text{Fe}_{x/2}\text{O}_2$  ( $x = 0.5$ ).

## 2. Experimental procedure

The starting raw materials were MgO [Alfa (Johnson Matthey), 96%], Fe<sub>2</sub>O<sub>3</sub> (Merck, 99%) and Nb<sub>2</sub>O<sub>5</sub> [Alfa (Johnson Matthey), 99.5%]. The samples were prepared by the conventional ceramic method by mixing with ethyl alcohol in an agate mortar for 4 hours. The

amounts of reagents were calculated according to the following equation

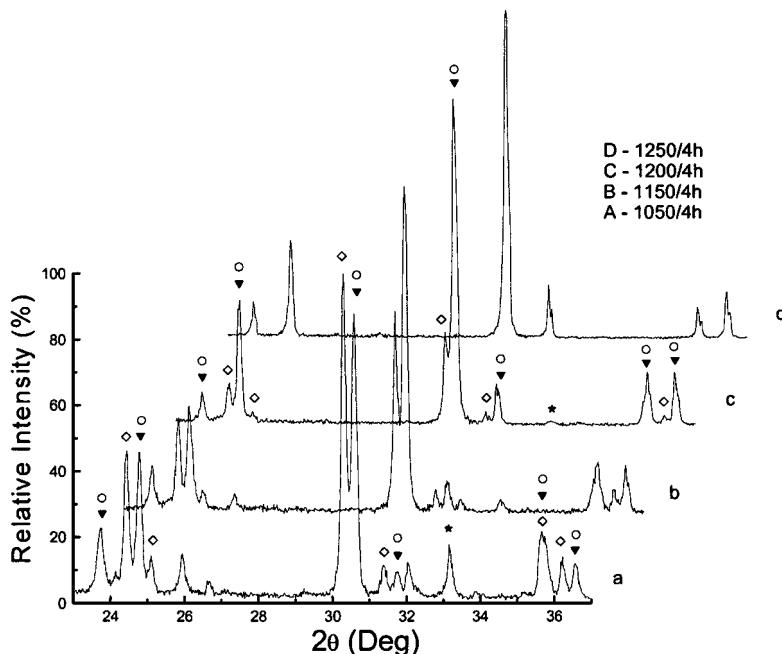
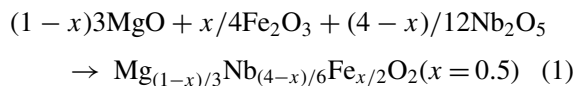


Figure 1 X-ray diffraction patterns of the Mg<sub>(1-x)/3</sub>Nb<sub>(4-x)/6</sub>Fe<sub>x/2</sub>O<sub>2</sub> (x = 0.5) powders calcined at different temperature, showing MgNb<sub>2</sub>O<sub>6</sub> (a), FeNbO<sub>4</sub> (b), [Fe, Mg]NbO<sub>4</sub> (c) and Fe<sub>2</sub>O<sub>3</sub> (d) phases.

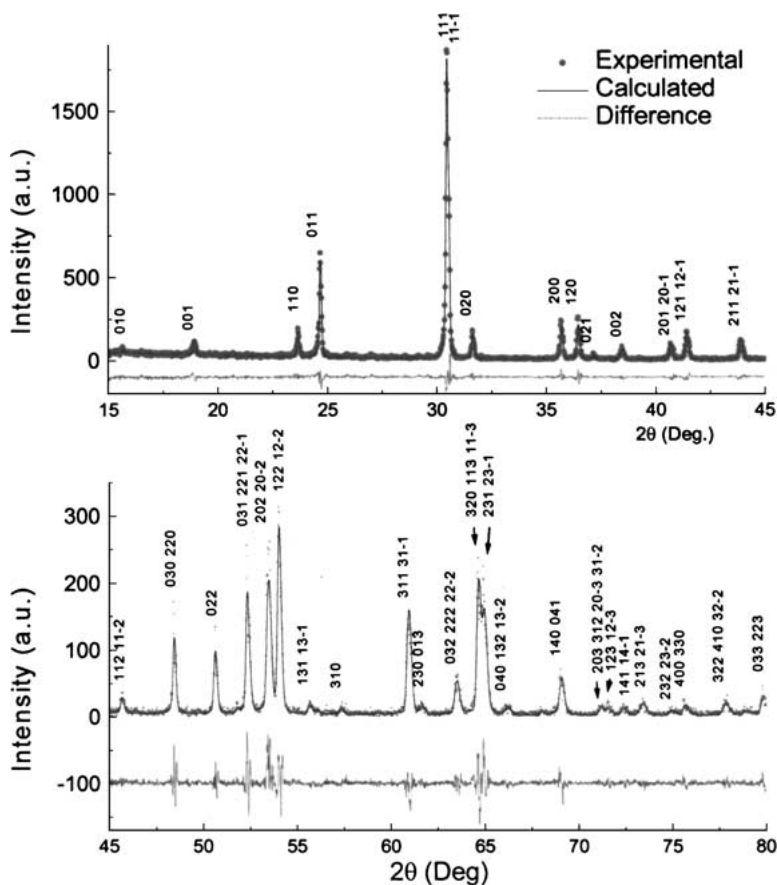


Figure 2 X-ray diffraction patterns of the Mg<sub>(1-x)/3</sub>Nb<sub>(4-x)/6</sub>Fe<sub>x/2</sub>O<sub>2</sub> (x = 0.5) powders calcined at 1200°C for 12 hours, showing the calculated profiles and the difference curve.

To study the phase composition and microstructural characteristics during the solid state reaction in the phase formation of  $\text{Mg}_{(1-x)/3}\text{Nb}_{(4-x)/6}\text{Fe}_x/2\text{O}_2$  ( $x = 0.5$ ), the powders were sintered at 1050, 1100, 1150, 1200 and 1250°C for 4 hours with heating and cooling rates of 5°C/min. All samples were examined by XRD using a Philips-PW-1821 diffractometer with  $\text{Cu K}_\alpha$  radiation (1.54056 Å). The patterns were scanned in  $2\theta$  from 10.01° to 79.99° with a 0.02°/1s step (3500 points). The microstructural analysis was

performed in a Jeol JSM 5300 scanning electron microscope with energy dispersive spectroscopy (EDS) attachment. Grain size was determined using Scion Image for Windows, version  $\beta$  4.02 software. The statistics were performed using a *fractional distribution function and length shape factor*.

### 3. Results and discussion

Fig. 1 shows representative XRD patterns of the powders calcined at different temperatures. In the early

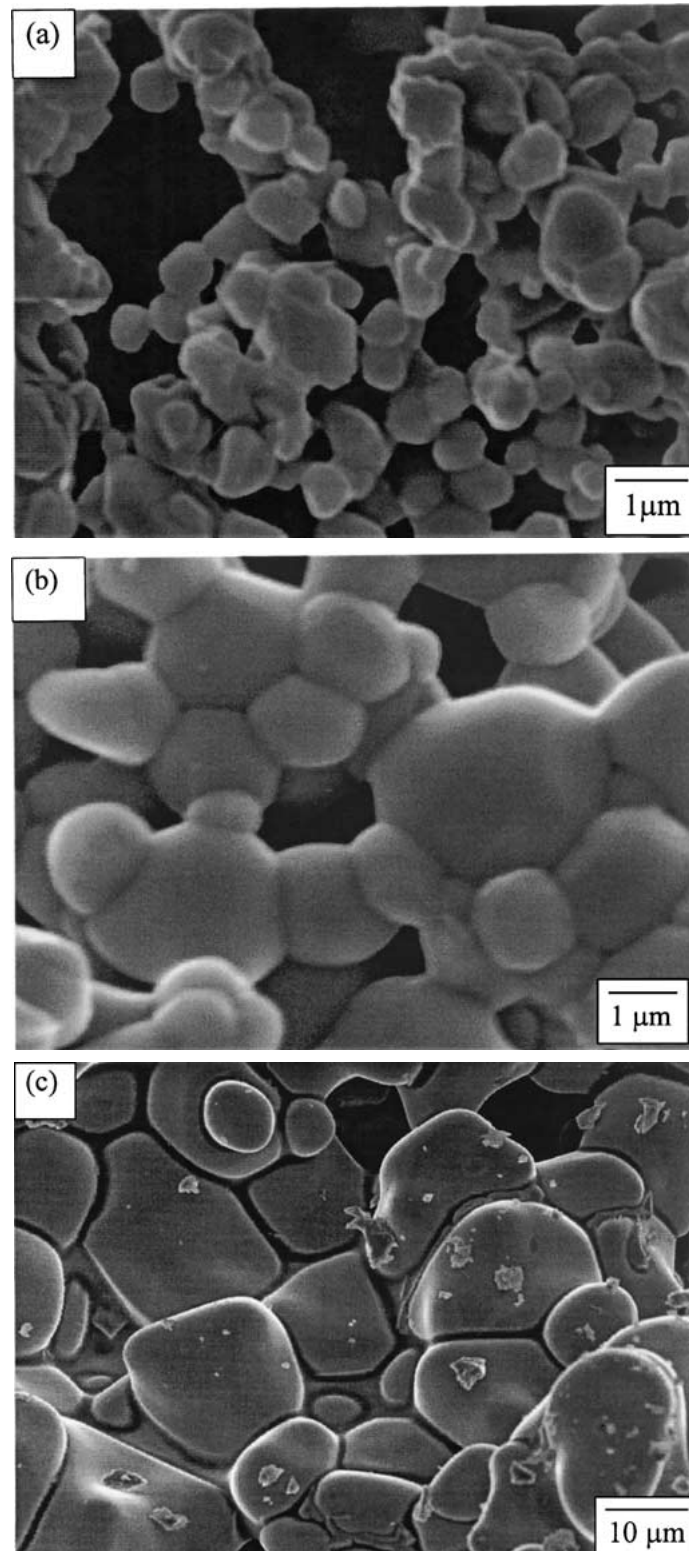


Figure 3 SEM micrographs of the  $\text{Mg}_{(1-x)/3}\text{Nb}_{(4-x)/6}\text{Fe}_x/2\text{O}_2$  ( $x = 0.5$ ) powders calcined at (a) 1050, (b) 1150 and (c) 1250°C for 4 hours.

stage of the reaction two dominant phases are clearly identified as magnocolumbite ( $\text{MgNb}_2\text{O}_6$ ) and ferrocolumbite ( $\text{FeNbO}_4$ ) as wolframites corresponding to JCPDS files 33-0875 and 71-1849 respectively.

Also, small amounts of  $\text{Fe}_2\text{O}_3$  (matched with JCPDS file 33-0664) and niobium oxides, which can be matched with JCPDS files 19-0859 and 19-0861, are present at  $1050^\circ\text{C}$  and disappear when the firing temperature increases. A detailed analysis of all patterns indicates the formation of a third significant phase at high temperatures, which became a single phase when heated at  $1200^\circ\text{C}$  for 12 hours. This phase did not match any JCPDS file and, as described below, was identified as  $[\text{Fe}, \text{Mg}]\text{NbO}_4$ , a wolframite.

The behavior of the strongest reflections around  $2\theta = 30.30^\circ$  and  $2\theta = 30.59^\circ$  is a good indicator of the phase transformation and the evolution of the solid state reaction. The peak centered at  $2\theta = 30.59^\circ$  can be connected with a superposition of the two wolframite-like phases mentioned above. At  $1050^\circ\text{C}$  (Fig. 1a), the pattern shows  $\text{MgNb}_2\text{O}_6$  as the majority phase as expected for these compounds at low sintering temperatures. For higher firing temperatures a significant change in the relative intensities of the diffraction peaks takes place (Fig. 1b–d). The notable reduction of the  $\text{MgNb}_2\text{O}_6$ ,  $\text{Fe}_2\text{O}_3$  and niobium oxide phases together with the shift to smaller angles of the characteristic peaks of the ferrocolumbites when the firing temperature increases, suggest the formation of a new single crystalline phase isostructural with the  $\text{FeNbO}_4$  where the Mg ions are incorporated in the new structure in the Fe ion sites.

Rietveld refinement was used for a more precise interpretation of the diffraction data corresponding to the sample fired at  $1200^\circ\text{C}$  for 12 hours using FULLPROF-98 software [19, 20]. From a preliminary analysis, the starting structure was a monoclinic cell, space group  $P1\ 2/a\ 1$ , with initial parameters  $a = 5.02\ \text{\AA}$ ,  $b = 5.65\ \text{\AA}$ ,  $c = 4.68\ \text{\AA}$  and  $\beta = 89.7^\circ$ . The atomic positions were the Wyckoff positions reported for  $\text{FeNbO}_4$  corresponding to ICSD 14015 [21].

According to the initial chemical composition, Fe and Mg ions were situated at the same site in such a manner that the Fe/Mg atomic ratio was 1.5 and a new chemical formula  $[\text{Fe}_{0.6}, \text{Mg}_{0.4}]\text{NbO}_4$  was satisfied. Diffraction peaks were described by a Thompson-Cox-Hasting pseudo-Voigt (TCH-pV) function. Fig. 2 shows the experimental and calculated profiles with the difference curve plotted at the bottom. As can be seen, the difference curve takes relatively high values at certain angles. This could be due to insufficient statistics of the diffraction dataset that do not allow good resolution particularly for some of the overlapped reflections [22]. However, the values of the statistical parameter  $\chi^2 = 1.71$  and the goodness of fit index  $\text{GoF} = 1.3$  are good indicators of a satisfactory agreement. The final cell parameters were  $a = 5.023(3)\ \text{\AA}$ ,  $b = 5.645(4)\ \text{\AA}$ ,  $c = 4.676(0)\ \text{\AA}$  and  $\beta = 89.8(7)^\circ$ . The use of the TCH-pV function allows an estimate of the microstrain and crystallite size. For microstrain, assuming the cell is pseudo-orthorhombic, a model of strain with fluctuations along  $a$ ,  $b$  and  $c$  and a correlation between parameters was employed. The calculated microstrain value

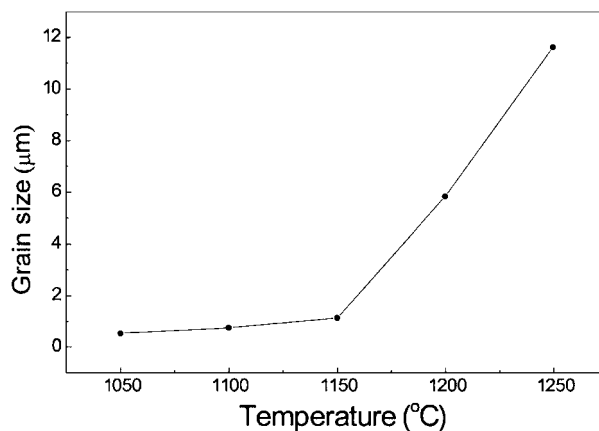


Figure 4 Average grain size of the calcined powders as a function of the calcination temperature.

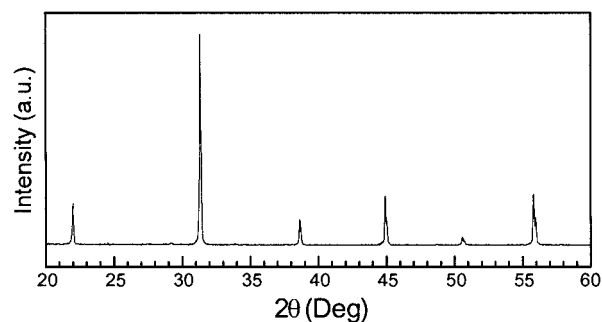


Figure 5 X-ray diffraction pattern of 0.5PMN-0.5PFN powder calcined at  $850^\circ\text{C}$  for 2 hours.

was about 0.3% for an isotropic Lorentzian contribution of the TCH-pV function. Crystallite size of approximately  $0.1\ \mu\text{m}$  was estimated for a Gaussian contribution. A detailed structural interpretation is in course and will be published elsewhere.

SEM micrographs of the powders sintered at different temperature are shown in Fig. 3. The particles are irregular in shape and the grain size tends to increase with calcination temperature. Fig. 4 shows the behavior of the average grain size as a function of the sintering temperature. It can be seen that for sintering temperatures above  $1150^\circ\text{C}$  an abrupt increase in the grain size takes place and the dispersion around the average value increases with grain size. This behavior suggests a new mechanism of grain growth that may be related to the formation of the new crystalline phase mentioned above.

The precursor powders described above were then mixed with stoichiometric amounts of  $\text{PbO}$  and calcined at  $700\text{--}950^\circ\text{C}$  for 4 hours to form the perovskite structure. Fig. 5 shows a representative XRD pattern of the calcined powders in which the perovskite structure is fully developed. No evidence of precursor phases was detected. It is concluded, therefore, that a pure PMN-PFN perovskite can be formed using  $[\text{Mg}, \text{Fe}]\text{NbO}_4$  as a precursor.

#### 4. Conclusions

The  $\text{MgNb}_2\text{O}_6$  columbite and iron niobium oxide ( $\text{FeNbO}_4$ ) were identified as intermediated compounds in the kinetic reaction to form  $[\text{Fe}, \text{Mg}]\text{NbO}_4$ . A new crystalline single phase was found, isostructural with

the FeNbO<sub>4</sub> type structure in the monoclinic phase. Shifts of the x-ray diffraction peaks to smaller angles were connected with the incorporation of magnesium in the new structure. From the preliminary analysis of XRD patterns it was possible to identify the phase as [Fe<sub>0.6</sub>, Mg<sub>0.4</sub>]NbO<sub>4</sub> of the space group P1 2/a 1 and with cell parameters  $a = 5.023(3)$  Å,  $b = 5.645(4)$  Å,  $c = 4.676(0)$  Å and  $\beta = 89.8(7)^\circ$ . The effectiveness of [Fe, Mg]NbO<sub>4</sub> as a precursor to obtain PMN-PFN was proven.

### Acknowledgments

This work was partially supported by CoNa-CyT (Proj.No.33586E) y DGAPA-UNAM (Proj. No. IN104000). Thanks are due to E. Aparicio and I. Gradilla for their technical assistance.

### References

1. Y. YAMASHITA, *Am. Ceram. Soc. Bull.* **73** (1994) 74.
2. R. E. WHATMORE, P. C. OSBOND and N. M. SHORROCKS, *Ferroelectrics* **76** (1987) 351.
3. T. R. SHROUT and A. HALLILAY, *J. Amer. Ceram. Soc. Bull.* **66** (1987) 704.
4. M. YOKOSUKA, *Jpn J. Appl. Phys.* **32** (1993) 1142.
5. X. S. GAO, X. Y. CHEN, J. YIN, J. WU and Z. G. LIU, *J. Mater. Sci.* **35** (2000) 5421.
6. T. HIDEKI, *J. Electr.* **4** (2000) 327.
7. F. CHAPUT, J. P. BOLITOT, M. LEJEUNE, R. PAPIERNIK and L. G. PFAIZGRAF, *J. Amer. Ceram. Soc.* **72** (1989) 1355.

8. M. M. A. SEKAR, A. HALLILAY and K. C. PATIL, *J. Mater. Res.* **11** (1996) 1210.
9. A. WATANABE, H. HANEDA, Y. MORIYOSHI, S. SHIRASAKI, S. KURAMOTO and H. YAMAMURA, *J. Mater. Sci.* **27** (1992) 1245.
10. Y. YOSHIKAWA and K. UCHINO, *J. Amer. Ceram. Soc.* **79** (1996) 2417.
11. S. M. GRUPTA and A. R. KULKARNI, *Mater. Chem. Phys.* **39** (1994) 98.
12. S. ANANTA and NOEL W. THOMAS, *J. Eur. Ceram. Soc.* **19** (1999) 2917.
13. SUN-GON JUN, NAM-KYOUNG KIM, JEONG-JOO KIM and SANG-HEE CHO, *Mater. Lett.* **34** (1998) 336.
14. S. L. SWARTZ and T. R. SHROUT, *Mater. Res. Bull.* **17** (1982) 1245.
15. B. H. LEE, N. K. KIM, B. O. PARK and S. H. CHO, *Mater. Lett.* **33** (1997) 57.
16. S. ANANTA and NOEL W. THOMAS, *J. Eur. Ceram. Soc.* **19** (1999) 155.
17. *Idem., ibid.* **19** (1999) 629.
18. *Idem., ibid.* **19** (1999) 1873.
19. RODRÍGUEZ-CARVAJAL, *J. Physica B* **192** (1993) 55.
20. *Idem., Reference Guide for the Computer Program FullProf.* Laboratoire Léon Brillouin, CEA-CNRS Saclay, France, 1996.
21. Inorganic Crystal Structure, ICSD data base. Release 1998.
22. L. B. MCCUSKER, R. B. VON DREELE, D. E. COX, D. LOVER and P. SCARTI, *Journal of Applied Crystallography* **32** (1999) 36.

*Received 5 December 2001  
and accepted 16 August 2002*